LA-UR- 12-00323

Approved for public release; distribution is unlimited.

Title:	Bond Strength Characterization of Plasma Sprayed Zirconium on Uranium Alloy by Microcantilever Testing
Author(s):	Kendall Hollis, Nathan Mara, Robert Field, Patricia Dickerson, Tom Wynn
Intended for:	2012 International Thermal Spray Conference, May 21-24, 2012, Houston, Texas

Form 836 (7/06)

Bond Strength Characterization of Plasma Sprayed Zirconium on Uranium Alloy by Microcantilever Testing

Kendall Hollis, Nathan Mara, Robert Field, Patricia Dickerson, Tom Wynn

Abstract

The future production of low enriched uranium nuclear fuel for test reactors requires a well adhered diffusion barrier coating of zirconium (Zr) on the uranium/molybdenum (U-Mo) alloy fuel. In this study, the interfacial bond between plasma sprayed Zr coatings and U-Mo fuel has been characterized for localized bond strength by microcantilever beam testing. Test results have revealed the effect of specific flaws such as cracks and pores on the bond strength of interfaces with a sampling area of approximately 20 μm^2. TEM examination has shown the Zr/U-Mo interface to contain rows of very fine grains (5-30 nm) with the Zr in contact with UO_2. Bond strengths of plasma sprayed samples have been measured that are similar to those of diffusion bonded samples showing the potential for plasma sprayed Zr coatings to have high bond strength.

Introduction

The US National Nuclear Security Administration Reactor Conversion Program mission supports the minimization and, to the extent possible, elimination of the use of highly enriched uranium in worldwide civil nuclear applications by working to convert research and test reactors to the use of low enriched uranium (LEU) fuel with a U-235 enrichment of less than 20%. The fuel under development consists of a center U-10%Mo foil (178-508 μm thick x 43.3-103 mm wide x 289-1219 mm long) encased in 6061 aluminum (Ref 1). One of the primary challenges in developing the LEU fuel is the insertion of a thin (25-60 μm) diffusion barrier to prevent the interaction of the U-Mo fuel with the Al cladding (Ref 2). The diffusion barrier must be of high density to prevent fission gas accumulation, must be well bonded to the underlying U-Mo fuel foil and must have a top surface which promotes strong adhesion to the Al cladding which is hot isostatic press bonded to the coated fuel foil (ref 3). The characterization of the interface between the U-Mo fuel and the Zr diffusion barrier coating is crucial to predicting the useful lifetime of the fuel under various burn up conditions. The goal of this study is to characterize the interface between plasma sprayed Zr and a U-Mo substrate by testing the interface strength and identifying the chemistry and phase of the materials present at the interface.

The bond strength of plasma sprayed coatings is typically determined using a standardized tensile test such as ASTM C 633. The coating to be tested is applied to the flat face of a right circular cylinder 25 mm in diameter and 38 mm long. The coating thickness must exceed 380 μm to prevent full penetration of the adhesive through the coating which invalidates the test results. This type of test is poorly suited to the Zr coated U-Mo under investigation here due to the thin coating and thin substrate. The substrate temperature for the thin U-Mo foil increases rapidly during spraying and can exceed 900°C during deposition (Ref 4). Using a substrate that is 38 mm thick instead of the actual foil thickness of 200-500 μm will significantly change the surface temperature and along with it the coating adhesive and cohesive strength. The Zr coating thickness at only 25-60 μm is much less than the suggested 380 μm test sample thickness so adhesive penetration and the associated uncertainties in bond strength measurements are a significant issue.

In order to address the challenges of bond strength testing of thin coatings on thin substrates, the micro-cantilever method of bond strength testing was chosen for this study (Ref 5). Very small cantilever beams with approximate cross section of 4 μm x 4 μm and length of 23 μm are produced by focused ion beam (FIB) milling of a sprayed sample to locate the coating/substrate interface near the base of the cantilever. A load is place on the free end of the cantilever using a nanoindenter to measure force and displacement. The actual geometry and loading location can be analyzed with a finite element model to determine the yield strength of the cantilever containing the bond (Ref 5). This technique allows traditional beam testing of samples (as opposed to multi-mode loading such as in scratch type testing) which are too thin for macro scale testing. In addition, bond strength is isolated to a small area allowing the study of the effect of single, specific flaws on the strength of the interface.

Experimental Procedure

Plasma spraying was conducted in a vacuum chamber in order to minimize the reaction of the Zr and U-Mo with the environment. The chamber was pumped down and back filled with Ar to 60 kPa (450 torr) for spraying. The plasma torch used was an SG-100 (Praxair, Indianapolis, Indiana, USA) with model 730 anode, 720 cathode and 112 gas injector. The primary gas was Ar at 40 standard liters per minute (slm), the secondary gas was He at 15 slm, the powder gas was Ar at 3 slm with powder feed rate of 5 g/min, the torch current was 850 A with voltage 28.6 V and the substrate standoff was 100 mm. Transferred arc cleaning at 20 A with the substrate negative was used before and during coating. The powder used was 99.2% minimum purity Zr (ATI Wah Chang, Albany, Oregon, USA). The powder was faceted in morphology with particle sizes ranging from 50 μm down to 5 μm. The substrate used was depleted uranium with 7 weight % Mo having dimensions 0.3 mm thick x 19 mm wide x 32 mm long. Prior to plasma spraying the substrate was cleaned in a 50% nitric acid solution and a nitric-HF solution was use for desmut. The samples were hot air dried which resulted in the visible formation of an oxide layer before being loaded into the spray chamber.

Microcantilevers were FIB machined (FEI Helios NanoLab 600 SEM/FIB, Hillsboro, Oregon, USA) to include the Zr coating/U-Mo substrate interface with the U-Mo forming the beam and the Zr forming the base. As shown in Figs. 1 and 5-3a, the interface was incorporated normal to the long axis of the microcantilevers, approximately 3-5 μm from the base, in order to subject it to tensile stresses. The cantilevers were cut to a pentagonal cross section as used in previous fracture studies (Ref 6), so that cracks would initially propagate with constant width. After milling, each cantilever was imaged using the same SEM/FIB before testing to allow the actual width and thickness to be measured.

Once the cantilevers were fabricated, they were tested using a nanoindenter (Agilent nanoXP, Santa Clara, California, USA) fitted with a Berkovich tip, where load and displacement data were acquired as a function of time. Quasistatic displacement rates of typically ~67 nm/second were chosen. The cantilevers were loaded at a location 5 μm from the cantilever free end. After testing, the cantilever was examined via SEM to locate the exact point of loading. The compliance associated with the indentation mark left in the end of the cantilever was subtracted from the overall displacement by using indentation data from the bulk of the material. The Zr/U-Mo interface before and after testing was characterized using TEM (FEI Tecnai F30 Analytical TEM/STEM, Hillsboro, Oregon, USA) techniques of imaging, selected area electron diffraction (SAD) and energy dispersive X-ray spectroscopy (EDS).

Results

The Zr coating on the U-Mo substrate is shown in Fig. 2. The coating is approximately 25 μm thick on average with a roughness typical of plasma sprayed material. The interface is rough but there is intimate contact between the coating and substrate for most of the length. Some porosity is visible in the coating as well as some porosity in the substrate near the coating interface. There is also a small amount of what appears to be U-Mo in the Zr coating near the interface as indicated in the SEM-back scattered electron image in Fig. 2.

Four microcantilever samples were machined from the Zr/U-Mo interface region and tested. The load/displacement results of these tests are shown in Fig. 3 and 4. Sample 1 and 2 reach a maximum load of only 0.79 mN and 0.63 mN respectively before fracture. Sample 3 was loaded to 3.17 mN without failure then unloaded while sample 4 reached a maximum of 4.03 mN before fracture. For comparison, results from microcantilever tests of 650°C diffusion bonded samples of Zr on U-Mo are also shown in Fig. 4.

SEM images of the samples before and after testing are shown in Fig. 5. Sample 1 failed very near the Zr/U-Mo interface. Prior to testing, a crack in the U-Mo near the interface is visible. This crack was likely the location of fracture initiation. Sample 2 before testing shows a pore in the U-Mo. Pores in the U-Mo are observed in Fig. 2 also and thought to be caused by vigorous displacement of molten substrate material during TA cleaning causing the encapsulation of pores. The fracture in sample 2 occurs at the Zr/U-Mo interface and extends through the U-Mo into the pore. The presence of the pore likely caused a stress concentration which lead to premature failure at the interface. Sample 3 with testing stopped prior to failure shows no discernable fracture. Sample 4 was tested to fracture and failed near the Zr/U-Mo interface. The fracture appears to have initiated on the U-Mo side of the interface and propagated through the U-Mo portion of the beam. In addition to the primary fracture location, strain localization regions (shear bands) appear in the U-Mo portion of the beam near the coating interface.

Low and high magnification TEM images of the plasma sprayed Zr/U-Mo interface in an untested sample are shown in Figs. 6 and 7. The interfacial zone appears to consist of a double layer of fine grains: a single layer of ~20-30 nm grains on the Zr side and multiple layers of 5-10 nm grains on the U-Mo side. SAD micro-diffraction patterns taken from grains on the Zr side are consistent with a <11-23> zone axis of hexagonal close-packed α-Zr and those taken on the U-Mo side with a <112> zone axis of cubic UO_2. EDS data taken in the same region is consistent with the identification of Zr and UO_2 as the materials in contact at the interface.

A TEM image of the fractured interface from sample 1 is shown in Fig. 8. The use of SAD and EDS identified the α-Zr, UO_2, γ-U and Pt phases in the figure. The Pt layer is deposited prior to FIB milling the TEM sample to protect the surface. During the FIB process, material removed can re-deposit on free surfaces not acted on by the ion beam. This re-deposited material is observed on the fracture surfaces of the sample. Fig. 8 shows that in the selected location, the fracture lies primarily between the Zr coating and the U substrate. However, the UO_2 in the upper part of the image is adhered to the Zr side rather than the U side indicating that the fracture has propagated between the U and the UO_2.

Discussion

The four microcantilever test sample results demonstrate the variety of information that can be learned about the interface between plasma sprayed coatings and their substrates. Sample 1 had a pre-existing crack-like flaw in the U-Mo at the top of the beam where the tensile force is greatest. The tensile fracture occurred along this flaw in the U-Mo and extended along the Zr/U-Mo interface. The low maximum force (0.79 mN) sustained by this flaw-containing interface demonstrates the effect of such a flaw on localized tensile bond strength. Sample 2 contained a large pore at the bottom of the sample near the interface in the U-Mo material. This sample also failed at a low maximum force (0.63 mN). The tensile fracture appears to have initiated at the Zr/U-Mo interface and propagated through the U-Mo material and into the pore. However, due to the presence of the pore, the location of maximum stress may have been below the top surface of the beam so that fracture initiation could have taken place at a location below the beam top surface. In either case, stress concentration on a smaller area due to the absence of material in the pore has resulted in a low strength interface.

Samples 3 and 4 showed no obvious flaws on the exterior of the beams prior to testing. Sample 3 was loaded to 3.17 mN without fracture then unloaded and returned back to near the starting strain. This indicates that the strain on the cantilever and interface was primarily elastic. No evidence of fracture was observed on the sample after testing. The shape of the load/displacement curve during loading is very similar to that of diffusion bonded sample 2. This indicates that in this specific test location, the bond strength character of the plasma sprayed and diffusion bonded samples are quite similar. Sample 4 was tested to failure with a maximum load of 4.03 mN. The load/displacement curve had a lower slope than sample 3 indicating that perhaps bonding took place over a smaller percentage of the total interface area for sample 4 compared to sample 3. The fracture took place near the interface in the U-Mo part of the beam. This suggests that the adhesive bond between the Zr and U-Mo is similar in strength to the cohesive U-Mo material strength near the interface. The occurrence of the fracture in the U-Mo may have been caused by the introduction of flaws in the substrate during TA cleaning as are observed in Figs. 2 and 5-2a. However, considering the interface of sample 4 may only be partially bonded and the strength of the U-Mo may have been reduced, the maximum load of 4.03 mN for sample 4 compares favorably to diffusion bonded samples 1 and 2 with maximum loads of 5.77 mN and 4.07 mN respectively. This result shows that plasma sprayed materials can have similar bond strength to diffusion bonded materials on a localized scale. Reduction of the flaws in plasma sprayed material is needed to bring the macro-scale bond strength up to that of diffusion bonded materials.

TEM observations of the Zr/U-Mo interface show a fine-grained structure on both the Zr and U side. The U side consists of a thin layer of UO_2 while the Zr side shows only α-Zr. Despite efforts to chemically etch and arc clean the oxide from the U-Mo surface, some UO_2 remains. This attests to the extremely high affinity for oxygen of uranium metal. The fracture surface of sample 1 viewed by TEM showed that crack propagation can take place between the Zr coating and U-Mo substrate but also can take place between the U-Mo and UO_2. This indicates that the Zr/UO_2 and the U-Mo/UO_2 bonds are similar in strength.

Summary Observations and Conclusions

The following observations and conclusions have resulted from this study.

Microcantilever beams have been successfully FIB milled from a plasma sprayed Zr coating on a U-Mo substrate.

Testing of the microcantilevers reveals strength differences in the region of the coating/substrate interface due to pre-existing flaws (cracks or pores).

Testing of samples without visible pre-existing flaws results in force/displacement values similar to diffusion bonded samples of the same materials. This indicates that if the frequency of flaws in the plasma sprayed coating is reduced, the bond strength may approach that of a diffusion bonded sample.

Evidence of a thin, fine-grained interface consisting of α-Zr and UO_2 was revealed by TEM.

The fracture surface for a sample with a pre-existing crack was primarily between the Zr and the U-Mo indicating an adhesive type failure but some evidence was found of fracture between the U-Mo and a UO_2 layer indicating that the Zr/UO_2 bond is similar in strength to the $U\text{-}Mo/UO_2$ bond.

Acknowledgement

The authors would like to acknowledge Ann Kelly for her help with metallographic preparation of samples and David Dombrowski for his review of the manuscript. This work was funded by the DOE NNSA Global Threat Reduction Initiative's Reactor Conversion Program.

References

1. D.M. Wachs, C.R. Clark, R.J. Dunavant, Conceptual Process Description for the Manufacture of Low-Enriched Uranium-Molybdenum Fuel, Idaho National Laboratory report INL/EXT-08-13840, Feb. 2008.
2. Hollis, K.J.: Zirconium Diffusion Barrier Coatings for Uranium Fuel used in Nuclear Reactors. Advanced Materials & Processes, 2010, **168**(11), p 57-9.
3. Hollis, K.J. and M.I. Pena: Plasma Sprayed and Electrospark Deposited Zirconium Metal Diffusion Barrier Coatings. *Thermal Spray: Global Solutions for Future Application*, DVS-ASM, May 2010, p 439/44.
4. K.J. Hollis, M.E. Hawley, P.O. Dickerson, Characterization of Thermal Diffusion Related Properties in Plasma Sprayed Zirconium Coatings, *J. Therm. Spray Technol.*, in press.
5. N.A. Mara, J. Crapps, T. Wynn, K. Clark, P. Dickerson, D.E. Dombrowski, B. Mihaila, A. Antoniou, Nanomechanical Behavior of U-10Mo/Zr/Al Fuel Assemblies, *Conference Proceedings of the 33rd International Meeting on Reduced Enrichment for Research and Test Reactors*, Oct. 23-27, 2011, Santiago, Chile.
6. D. Di Maio, S.G. Roberts, Measuring Fracture Toughness of Coatings Using Focused-Ion-Beam-Machined Microbeams, *J. Mater. Res.*, 2005, **20**(2), p 299-302.

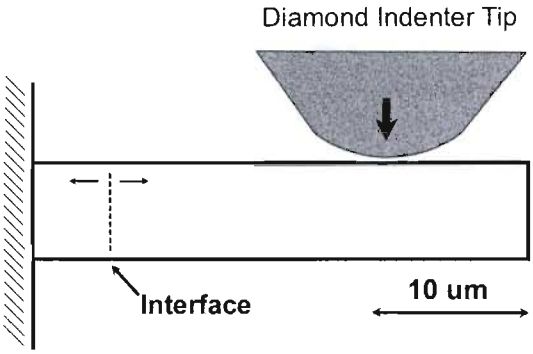

Figure 1: Schematic of microcantilever test configuration.

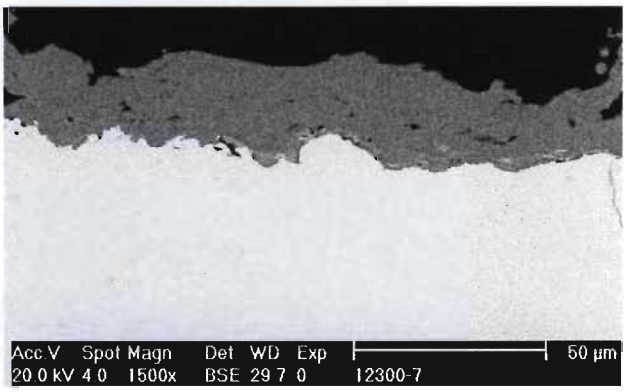

Figure 2: SEM back scattered electron image showing Zr coating (gray) on U-Mo substrate (white).

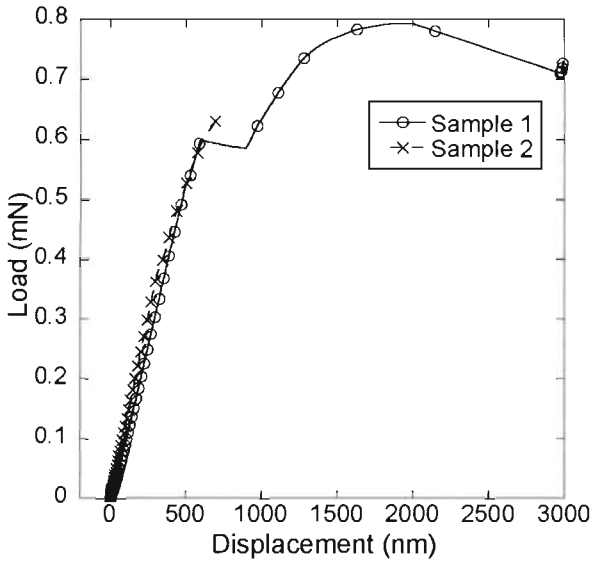

Figure 3: Load displacement curve for microcantilever samples 1 and 2.

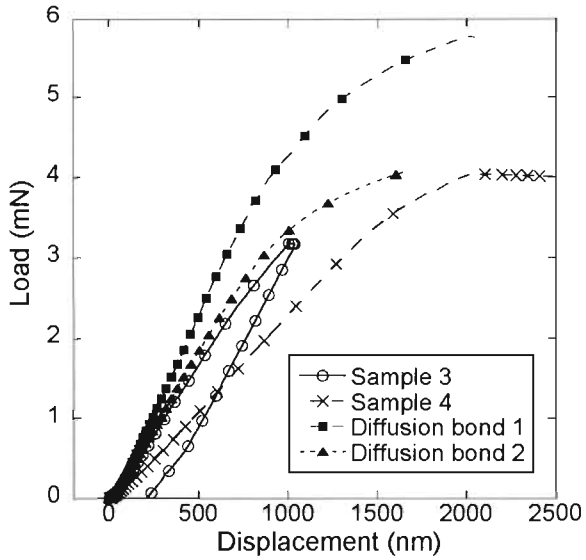

Figure 4: Load displacement curve for microcantilever samples 3 and 4 along with representative diffusion bonded samples.

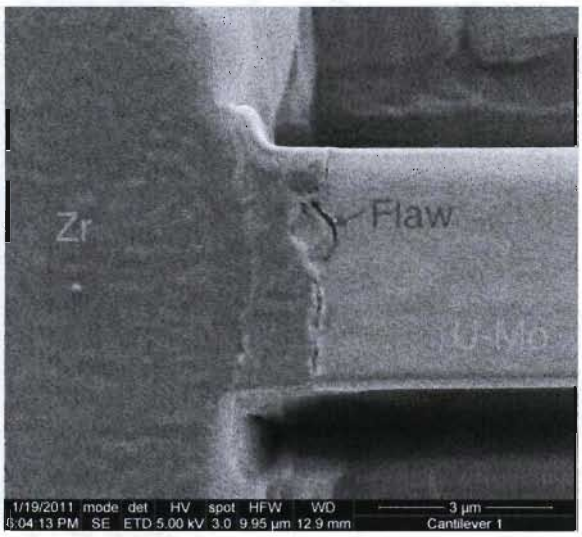

Figure 5-1a: The base of the cantilever of sample 1 before testing.

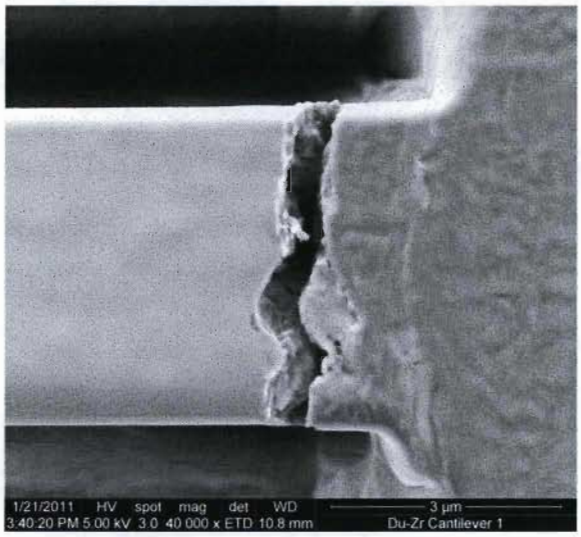

Figure 5-1b: Sample 1 after fracture.

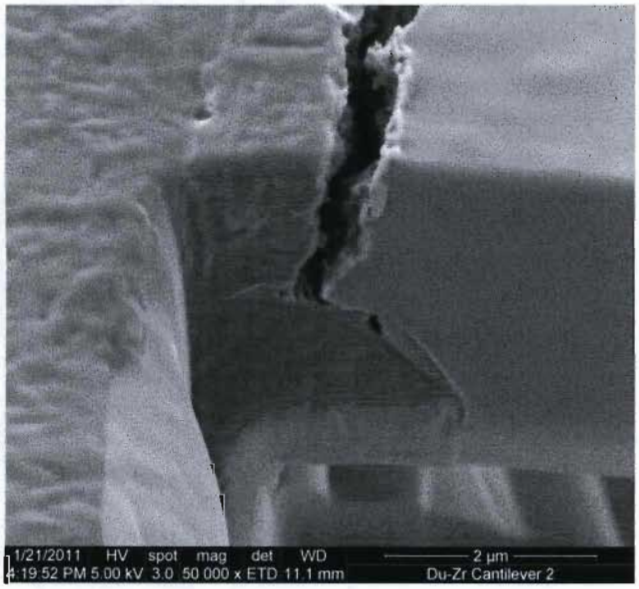

Figure 5-1c: Side view of sample 1 after testing.

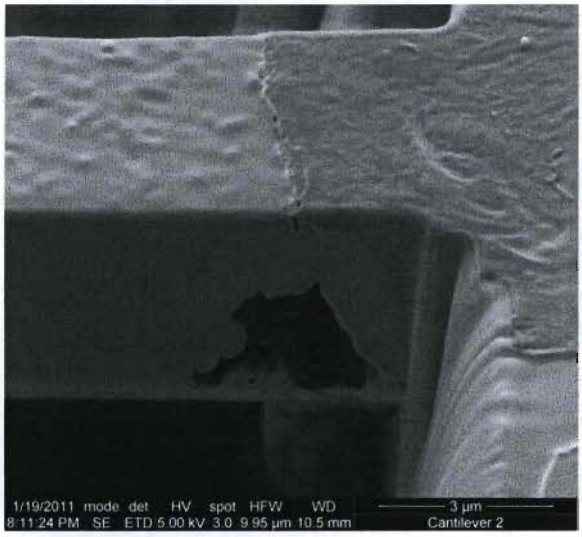

Figure 5-2a: Side view of the base of the cantilever of sample 2 before testing.

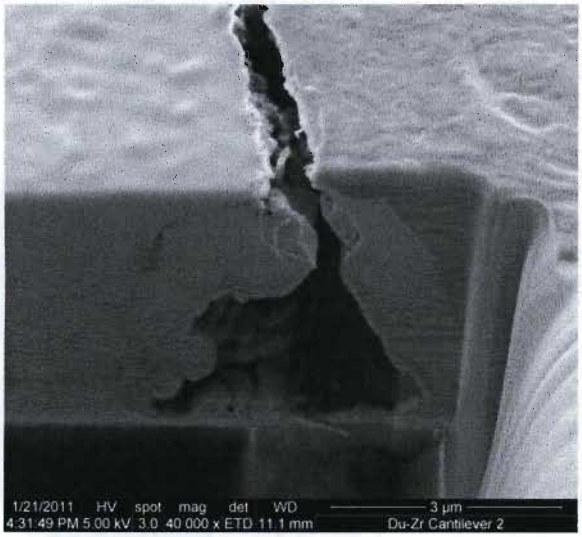

Figure 5-2b: Sample 2 after fracture.

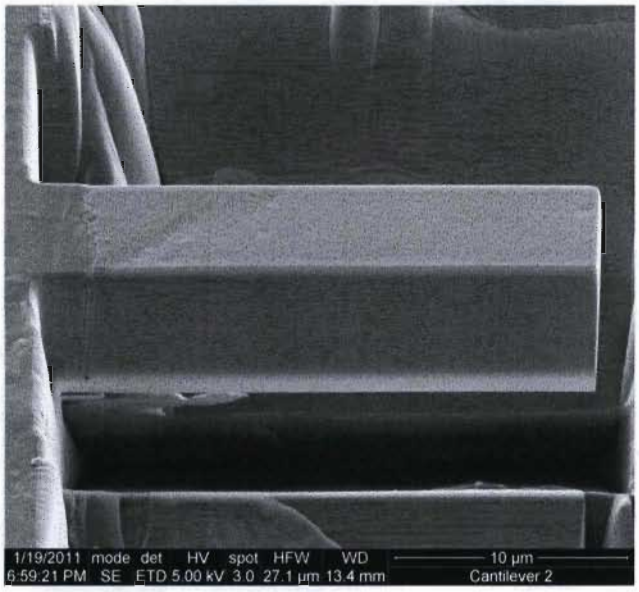

Figure 5-3a: Full cantilever view of sample 3 before testing.

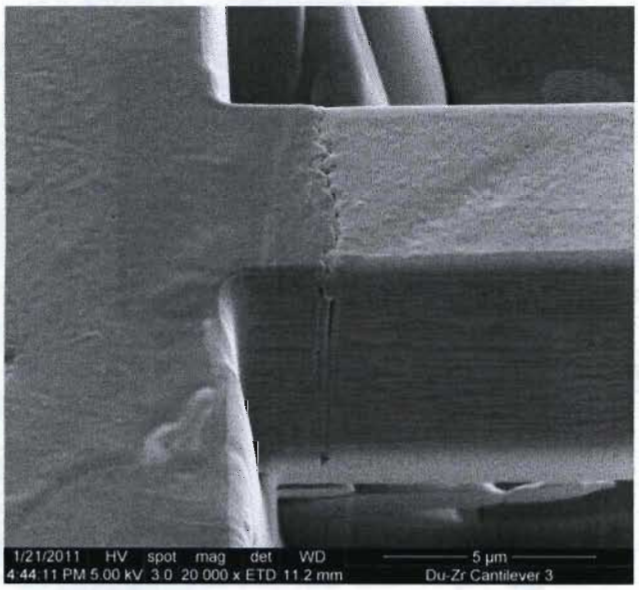

Figure 5-3b: Sample 3 after testing with release of load before fracture.

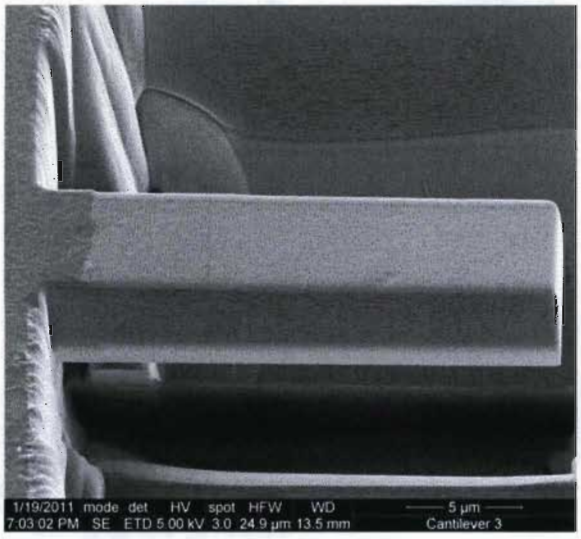

Figure 5-4a: Sample 4 before testing.

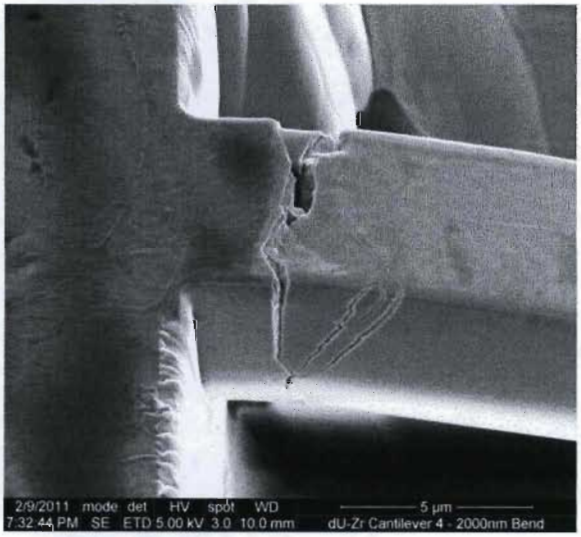

Figure 5-4b: Sample 4 after fracture with shear bands in the U-Mo.

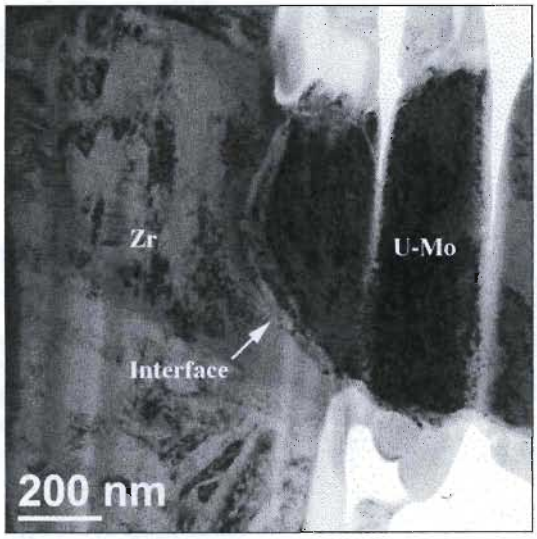

Figure 6: TEM image of the Zr/U-Mo interface of an untested coating.

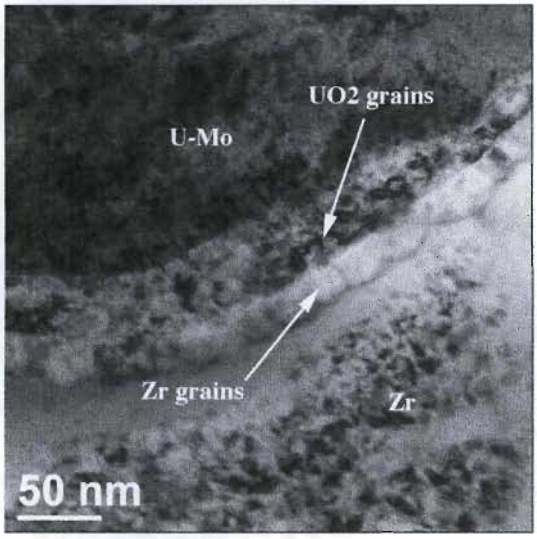

Figure 7: TEM high magnification image of the Zr/U-Mo interface.

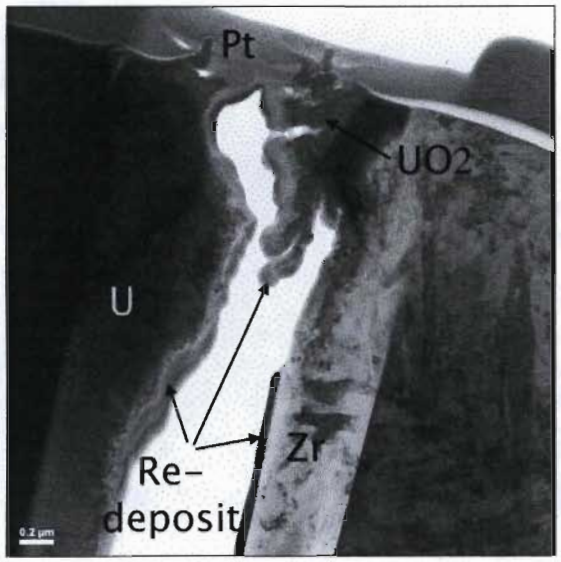

Figure 8: TEM image of the fracture surface of sample 1 after microcantilever testing.